



**HAL**  
open science

## **Oncolytic rat parvovirus H-1PV, a candidate for the treatment of human lymphoma: In vitro and in vivo studies.**

Assia L Angelova, Marc Aprahamian, Ginette Balboni, Henri-Jacques Delecluse, Regina Feederle, Irina Kiprianova, Svitlana P Grekova, Angel S Galabov, Mathias Witzens-Harig, Anthony D Ho, et al.

### ► To cite this version:

Assia L Angelova, Marc Aprahamian, Ginette Balboni, Henri-Jacques Delecluse, Regina Feederle, et al.. Oncolytic rat parvovirus H-1PV, a candidate for the treatment of human lymphoma: In vitro and in vivo studies.. *Molecular Therapy*, 2009, 17 (7), pp.1164-72. 10.1038/mt.2009.78 . pasteur-00748227

**HAL Id: pasteur-00748227**

**<https://riip.hal.science/pasteur-00748227v1>**

Submitted on 5 May 2013

**HAL** is a multi-disciplinary open access archive for the deposit and dissemination of scientific research documents, whether they are published or not. The documents may come from teaching and research institutions in France or abroad, or from public or private research centers.

L'archive ouverte pluridisciplinaire **HAL**, est destinée au dépôt et à la diffusion de documents scientifiques de niveau recherche, publiés ou non, émanant des établissements d'enseignement et de recherche français ou étrangers, des laboratoires publics ou privés.

# Oncolytic Rat Parvovirus H-1PV, a Candidate for the Treatment of Human Lymphoma: *In Vitro* and *In Vivo* Studies

Assia L Angelova<sup>1,2</sup>, Marc Aprahamian<sup>3</sup>, Ginette Balboni<sup>3</sup>, Henri-Jacques Delecluse<sup>4</sup>, Regina Feederle<sup>4</sup>, Irina Kiprianova<sup>1</sup>, Svitlana P Grekova<sup>3</sup>, Angel S Galabov<sup>2</sup>, Mathias Witzens-Harig<sup>5</sup>, Anthony D Ho<sup>5</sup>, Jean Rommelaere<sup>1</sup> and Zahari Raykov<sup>1</sup>

<sup>1</sup>Programme Infection and Cancer, Tumor Virology Division and Institut National de la Santé et de la Recherche Médicale (INSERM) Unit 701, German Cancer Research Center (DKFZ), Heidelberg, Germany; <sup>2</sup>Department of Virology, The Stephan Angeloff Institute of Microbiology, Bulgarian Academy of Sciences, Sofia, Bulgaria; <sup>3</sup>Institut National de la Santé et de la Recherche Médicale (INSERM) Unit 701 and Institut de Recherche contre les Cancres de l'Appareil Digestif (IRCAD), Strasbourg, France; <sup>4</sup>Programme Infection and Cancer, Pathogenesis of Virus-Associated Tumors Division, German Cancer Research Center, Heidelberg, Germany; <sup>5</sup>Medizinische Universitäts-Klinik und Poliklinik, Innere Medizin V, Heidelberg, Germany

The incidence of lymphomas developing in both immunocompetent and immunosuppressed patients continues to steadily increase worldwide. Current chemotherapy and immunotherapy approaches have several limitations, such as severe side toxicity and selection of resistant cell variants. Autonomous parvoviruses (PVs), in particular the rat parvovirus H-1PV, have emerged as promising anticancer agents. Although it is apathogenic in humans, H-1PV has been shown to infect and suppress various rat and human tumors in animal models. In this study, we demonstrate the capacity of H-1PV for efficiently killing, through necrosis, cell cultures originating from Burkitt's lymphoma (BL), while sparing normal B lymphocytes. The cytotoxic effect was generally accompanied by a productive H-1PV infection. Remarkably, parvovirus-based monotherapy efficiently suppressed established BL at an advanced stage in a severe combined immunodeficient (SCID) mouse model of the disease. The data show for the first time that an oncolytic parvovirus deserves further consideration as a potential tool for the treatment of some non-Hodgkin B-cell lymphomas, including those resistant to apoptosis induction by rituximab.

Received 5 November 2008; accepted 23 March 2009; published online 14 April 2009. doi:10.1038/mt.2009.78

## INTRODUCTION

Epstein-Barr virus (EBV), a lymphotropic  $\gamma$ -herpes virus found in the human population worldwide, is characterized by its unique ability to efficiently transform normal resting B lymphocytes *in vitro* converting them into lymphoblastoid cell lines (LCLs). *In vivo*, the virus is strongly associated with the heterogeneous group of non-Hodgkin lymphomas (NHLs) [endemic and nonendemic Burkitt's lymphoma (BL), immunoblastic B-cell lymphomas in immunodeficient patients, among

others], and Hodgkin lymphoma (HL).<sup>1,2</sup> Current chemotherapy of lymphomas relies on several combined cyclophosphamide-, cisplatin-, and adriamycin-based regimens. Most of the drugs exert short- or long-term toxic effects, thus substantially affecting patients' quality of life.<sup>3</sup> Immunotherapy with rituximab, a chimeric humanized anti-CD20 monoclonal antibody (Rituxan), alone or in combination with chemotherapy, has significantly improved the treatment outcome in NHL patients. However, some patients become ultimately unresponsive or relapse through a mechanism that has not yet been clarified.<sup>4</sup>

Novel approaches are clearly needed, as first- or second-line treatments, for the efficient control of human lymphoid malignancies. In this regard, autonomous rodent parvoviruses (PVs) have emerged as promising anticancer agents.<sup>5</sup> These oncolytic agents are endowed with a natural oncoselectivity, which appears to result, at least in part, from the dependence of viral DNA replication,<sup>6</sup> gene expression,<sup>7</sup> and nonstructural protein cytotoxic activity<sup>8</sup> on the proliferation and transformation of host cells. Accumulation of NS1, the major viral nonstructural protein, was shown to be the primary cause of parvovirus-driven oncolysis.<sup>9</sup> In particular, it has been shown in our laboratory that the rat parvovirus H-1PV selectively kills several human tumor-derived cell lines.<sup>10-13</sup> Moreover, H-1PV systemic or intratumoral injection leads to suppression of various human carcinoma cell-derived tumors in animal models.<sup>14-16</sup> Importantly, H-1PV is infectious but devoid of significant pathogenicity for humans.<sup>17</sup>

It was previously shown that cell transformation by oncogenic viruses enhances permissiveness for H-1PV infection and, in particular, that some transformed human lymphoid cells can be parvovirus targets.<sup>18,19</sup> Based on these data, we initiated a larger screening of a panel of BL- and HL-derived or *in vitro* EBV-transformed LCLs with the aim to evaluate their sensitivity to H-1PV-induced killing. BL cells were distinguishable from the others by their especially high sensitivity to H-1PV, even after they had lost the EBV genome. EBV-positive BL cells were shown to

The last two authors contributed equally to this work.

Correspondence: Jean Rommelaere, Programme Infection and Cancer, Tumor Virology Division and Institut National de la Santé et de la Recherche Médicale (INSERM) Unit 701, German Cancer Research Center (DKFZ), Heidelberg 69120, Germany. E-mail: j.rommelaere@dkfz.de

die predominantly through necrosis, and killing was due to the parvovirus and not due to EBV lytic replication. Furthermore, important safety issues were addressed by demonstrating a low-level H-1PV toxicity for normal peripheral blood B cells stimulated to proliferate *in vitro* through lipopolysaccharide treatment. The efficiency of H-1PV inoculation as a monotherapeutic approach was confirmed in a severe combined immunodeficient (SCID) mouse model of established B-cell lymphoma xenografts.

## RESULTS

### BL-derived cell lines are highly sensitive targets for H-1PV-induced oncolysis *in vitro*

In order to determine the toxicity of H-1PV for lymphoma-derived or *in vitro* EBV-immortalized cell lines (LCLs), a panel of BL cells (Namalwa, Raji, Elijah, RAMOS, RAMOS-AW, RAMOS-EHRB, Akata), HL cells (L540, KM-H2, and HDLM2), and LCLs [Naive N17(8)/Memory M9(8), Naive N3(20)/Memory M1(20), JM, and 2089] was used. Cell cultures were infected with wild-type H-1PV at increasing multiplicities of infection, from 0.1 to 100 plaque-forming units (pfu)/cell, and cell viability was assessed using the Trypan blue dye exclusion test at 24-, 48-, and 72-hours postinfection (hpi). As shown in **Figures 1** and **2**, H-1PV induced a virus dose-dependent death in all cell lines tested. The killing effect augmented with time postinfection, to culminate, at 72 hpi, in 80–100% death of infected Namalwa, Raji, Elijah, RAMOS, and Akata cells (**Figure 1**). In contrast to these BL-derived lines, the LCLs [Naive N17(8)/Memory M9(8), Naive N3(20)/Memory M1(20), 2089], and two of the HL cells (KM-H2 and HDLM2) were less efficiently killed by H-1PV, with ~50% of the population remaining viable at 72 hours after infection at the highest multiplicity of infection (**Figure 2**). It is noteworthy that no B cell phenotype-related differences in H-1PV sensitivity were observed between *in vitro* EBV-transformed naive and memory B cells deriving from the same donor (**Figure 2a,d** and **b,e** for donors 8 and 20, respectively).

In order to assess whether the cytotoxic viral protein NS1 was expressed in the cell lines of interest, cultures were inoculated with a defective (but DNA replication-competent) H-1PV vector (chi-H-1PV/EGFP) in which the enhanced green fluorescence protein (EGFP), cDNA, substitutes for the sequence encoding the capsid proteins. In this construct, the P38 viral promoter driving EGFP expression is transactivated by NS1. It can thus be used to determine the capacity of cells for taking virus up and sustaining the replication phase of the viral life cycle. The fluorescent signal was detected in all cell lines tested at 24 hpi (**Supplementary Figure S1a–c**), and the fraction of NS1-positive cells in the respective lines was in proportion to their sensitivity to H-1PV infection, in keeping with the eventual death of lymphoma cells expressing the viral protein.

### Normal B cells from healthy donors are resistant to H-1PV infection

An important safety concern was whether normal B lymphocytes might be susceptible to H-1PV infection. To address this issue, we isolated B cells from the peripheral blood of healthy donors ( $n = 3$ ) and, after *in vitro* lipopolysaccharide stimulation, infected the cells with H-1PV. Trypan blue tests, further confirmed by methyl tetrazolium salt cytotoxicity assays, showed that H-1PV treatment of actively dividing normal B lymphocytes resulted in very low toxicity levels, not exceeding 20% of the population, even at the highest multiplicity of infection used (100 pfu/cell) (**Figure 3a**). After infection with chi-H-1PV/EGFP, fluorescence was not detected in any donor case, at 24 hpi (**Supplementary Figure S1d**) or later, suggesting that the observed mild toxicity was not directly related to viral gene expression. Because normal memory B cells are the most relevant counterparts of malignant BL and HL cells, it was further tested whether H-1PV infection of CD20<sup>+</sup>/CD19<sup>+</sup> B lymphocytes from healthy donors ( $n = 2$ ) caused any change in the fraction of these cells displaying the CD19<sup>+</sup>/CD27<sup>+</sup> memory phenotype. As shown in **Figure 3b**, no significant drop in the subpopulation of normal memory B lymphocytes

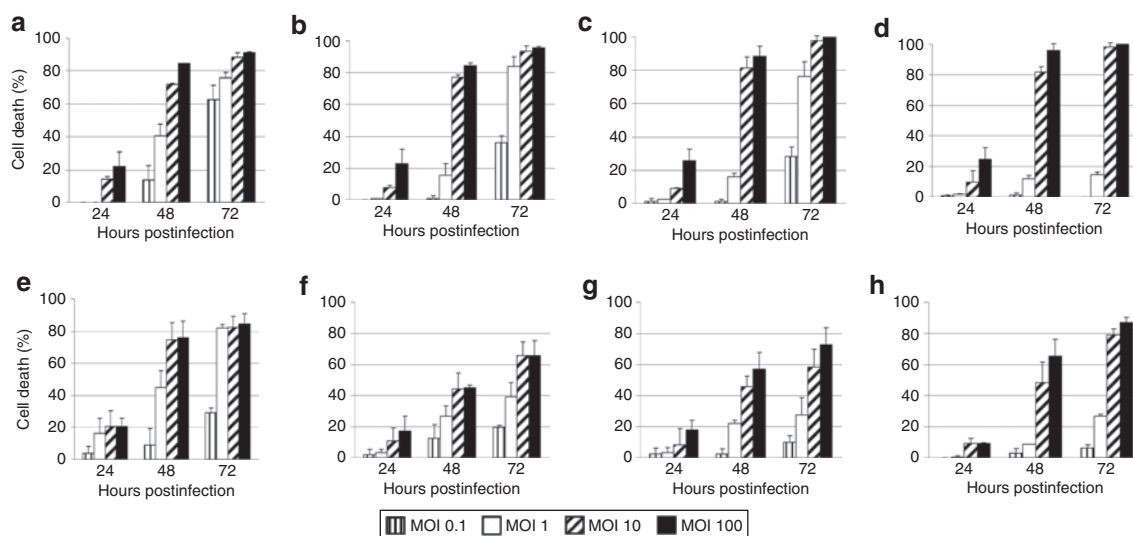


**Figure 1** Sensitivity of BL-derived cell lines to H-1PV-induced killing. (a) Namalwa, (b) Raji, (c) parental Elijah, (d) EBV-negative Elijah, (e) RAMOS, (f) RAMOS-AW, (g) RAMOS-EHRB, and (h) Akata cultures were infected with wild-type H-1PV (MOIs ranging from 0.1 to 100 pfu/cell). Cell viability was determined using the Trypan blue dye exclusion test at 24-, 48-, and 72-hours postinfection. Data are presented as percentage of cell death relative to the mock-treated controls. MOI, multiplicity of infection.

was detected after H-1PV treatment, irrespective of their proliferation status, confirming the overall resistance of these cells to H-1PV infection.

### H-1PV infection of BL lines is productive and leads to predominantly necrotic cell death

Monomeric and dimeric viral DNA replicative forms were detected by Southern blot analysis of H-1PV-infected cultures (data not shown), confirming that active parvoviral DNA replication was taking place in all cell lines. Production of infectious progeny particles, an important prerequisite for the therapeutic efficacy of oncolytic viruses, was further measured. Out of the 17 cell lines studied 11 (65%) sustained production of detectable amounts of H-1PV progeny virions (Table 1). BL-derived Namalwa, Raji, and Akata cells were found to be especially strong producers. The HL-derived KM-H2 and HDLM2 cell lines, which were less efficiently killed by the virus (Figure 2h,i) were still able to produce low levels of H-1PV progeny.

Given their high sensitivity to H-1PV, Namalwa cells were used to further investigate the cytopathic changes triggered by parvovirus infection in this system. Hoechst 33342 staining was first performed to detect alterations in nuclear morphology. Fluorescence microscopy examination of cultures at different time-points after infection revealed nuclear swelling and extensive DNA release from the nucleus into the cytosol, indicating that most cells died of necrosis (Figure 4a). However, at 48 hpi a few cells showed

nuclear fragmentation (Figure 4a, arrows), pointing to the fact that a minor fraction of the culture may undergo apoptosis. These results were confirmed by propidium iodide/Annexin-V staining of infected Namalwa cells (Figure 4b). The percentage of necrotic cells significantly increased between 24 (27.71%) and 48 (80.76%) hpi, whereas the apoptotic fraction was very low (<2%) and did not augment with time postinfection.

### H-1PV does not reactivate EBV in latently infected cells

It was important to ascertain that the cytopathic effects observed after exposure of EBV-positive cells to H-1PV, did not result from EBV lytic replication. We therefore stained parvovirus-infected Akata (Figure 4c) and Namalwa (data not shown) cells with an antibody specific for either BZLF1, an EBV immediate-early transactivator that initiates the lytic cycle, or gp350/220, an EBV envelope glycoprotein. Akata cells treated with an anti-immunoglobulin G ( $\alpha$ -IgG) antibody, known to induce EBV reactivation, were used as a positive control. No signs of initiation (BZLF1 expression) or completion (gp350/220 expression) of the EBV lytic cycle could be detected, upon H-1PV infection, in either of the two cell lines.

### *In vivo* established lymphomas are targets for H-1PV replication and cytopathic effects

Tumors were generated in SCID mice through subcutaneous injection of Namalwa cells. Tumors appeared in 100% of the

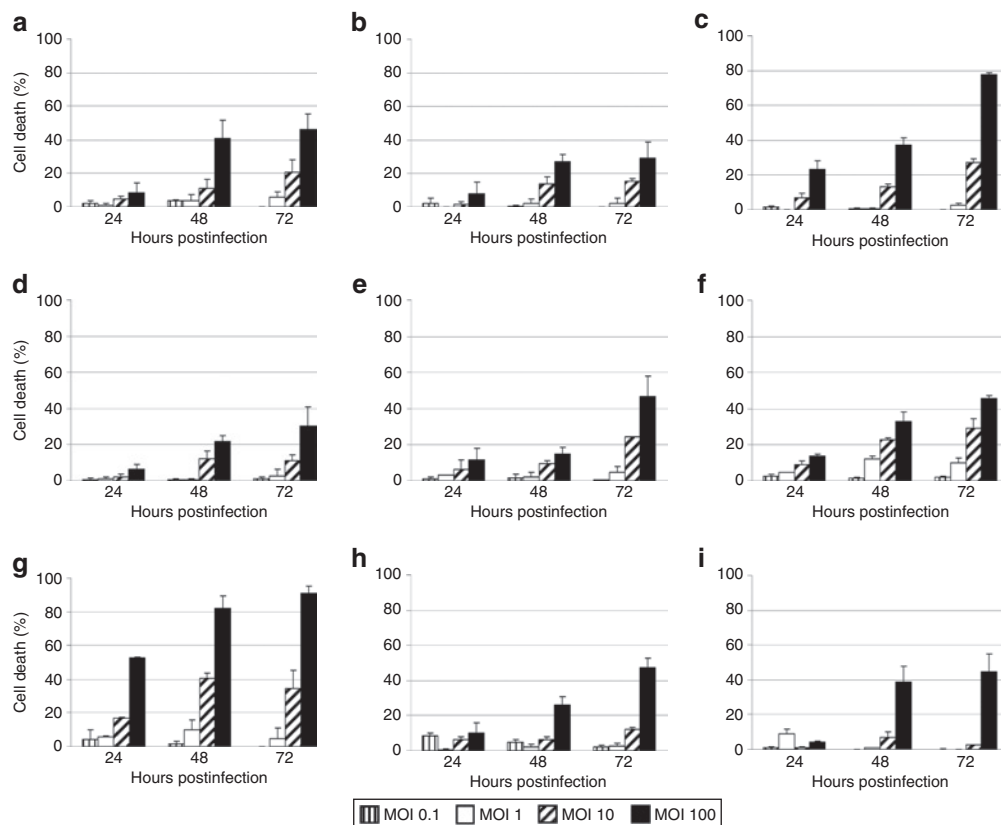
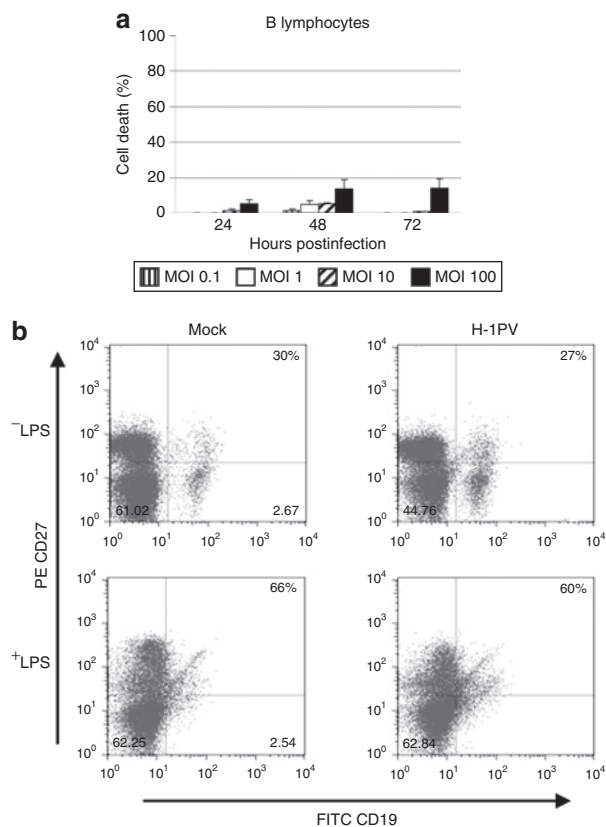


Figure 2 Sensitivity of LCLs and HL-derived cell lines to H-1PV-induced killing. The LCLs (a) Naive N17(8), (b) Naive N3(20), (c) JM, (d) Memory M9(8), (e) Memory M1(20), and (f) 2089, and the HL-derived cells (g) L540, (h) KM-H2, and (i) HDLM2, were infected with H-1PV, and processed as described in the legend to Figure 1.



**Figure 3** Sensitivity of normal peripheral blood B cells to H-1PV-induced killing. **(a)** Normal peripheral blood B cells were isolated from healthy donors ( $n = 3$ ), LPS-stimulated to proliferate *in vitro*, infected with wild-type H-1PV, and analyzed for the induction of cell death as described in the legend to **Figure 1**. **(b)** Peripheral blood mononuclear cells (PBMCs) were isolated from healthy donors ( $n = 2$ ), LPS-stimulated, and either infected with H-1PV (10 pfu/cell) or left untreated. At 48-hours postinfection, cells were harvested and processed for fluorescence-activated cell sorting analysis of CD20, CD19, and CD27 expression. The percentages of CD19<sup>+</sup>/CD27<sup>+</sup> (memory) B cells relative to the total CD20<sup>+</sup>/CD19<sup>+</sup> population are indicated.

animals in 14–17 days after cell inoculation, and were characterized by an extremely aggressive growth pattern, reaching a significant size (up to 3 cm<sup>3</sup>) within 15 days after becoming palpable. The tumors invaded the adjacent skeletal muscles and skin, with no evidence for distant spread, and appeared under microscopic examination as a high-grade lymphoma of the Burkitt type. Palpable tumors were treated with either ultraviolet (UV)-inactivated or infectious H-1PV. Viral DNA transcription (**Figure 5a**) and replication (**Figure 5b**) were measured at 7 days postinoculation and could only be detected in the infectious virus-treated tumors (compare UV.H-1PV and H-1PV lanes), indicating that the lymphoma cells sustained the parvovirus life cycle not only *in vitro* but also under *in vivo* conditions. Virus spreading to distant lymphomas was tested in mice bearing double tumors generated through Namalwa inoculation into each flank. To this end, one of the tumors was injected with H-1PV (**Figure 5a**, T1, T2), whereas the contralateral one remained untreated (**Figure 5a**, UT1, UT2). Viral expression was found to take place in both tumors, pointing to the ability of the virus to reach remote tumor sites.

**Table 1** Production of H-1PV progeny virions by lymphoma-derived and *in vitro* EBV-transformed lymphoblastoid cell lines

Cell line	Virus multiplication <sup>a</sup> (72-hpi titer/12-hpi titer)	Capacity for virus production
BL		
Namalwa	4,000	High
Raji	850	High
Elijah (+)	27	Moderate
Elijah (-)	2	Weak
RAMOS	44	Moderate
RAMOS-AW	57	Moderate
RAMOS-EHRB	30	Moderate
Akata	100	High
LCL		
JM	3	Weak
2089	0.8	No
Naive N17(8)	0.9	No
Memory M9(8)	1	No
Naive N3(20)	1	No
Memory M1(20)	0.7	No
HL		
L540	1	No
KM-H2	3.3	Weak
HDLM2	10	Weak

*Abbreviations:* BL, Burkitt's lymphoma; HL, Hodgkin lymphoma; hpi, hours postinfection; LCL, lymphoblastoid cell line.

<sup>a</sup>Amplification of taken up virus within 3 days after infection at a MOI of 0.1 pfu/cell.

H-1PV activity within the tumors was additionally confirmed by measuring the expression of NS1, the cytotoxic viral replicator protein (**Figure 5c**) and identifying pathological alterations in the neoplastic tissues. Hematoxylin–eosin staining of tumor slices processed 7 days after virus inoculation revealed large necrotic areas within infectious H-1PV-treated tumors (**Figure 5d**, hematoxylin–eosin staining). These histopathological signs were clearly absent when UV-inactivated H-1PV was used and correlated with NS1 expression within the tumor, as revealed by immunohistochemical detection of the protein (**Figure 5d**, IHC-NS1).

### H-1PV inoculation results in the regression of Namalwa tumors

In another setup of experiments, SCID mice carrying Namalwa cell xenografts were further used to evaluate the therapeutic efficiency of H-1PV monotherapy in an animal model of EBV-positive B-cell lymphoma. Two independent experiments were performed with the aim of evaluating the curative potential of H-1PV in early (tumor size 0.5 cm<sup>3</sup>) and advanced (tumor size 1–2 cm<sup>3</sup>) disease. In the early treatment protocol (**Figure 6a,b**), a virus dose of 10<sup>7</sup> pfu/animal was inoculated as a single intratumoral injection on day 14 after tumor initiation. The tumors in the control animals showed progressive growth within 15 days after inoculation of UV-inactivated virus, and mice were killed at this stage of the disease. In contrast, the infectious H-1PV-treated group experienced drastic tumor regression within 30 days after

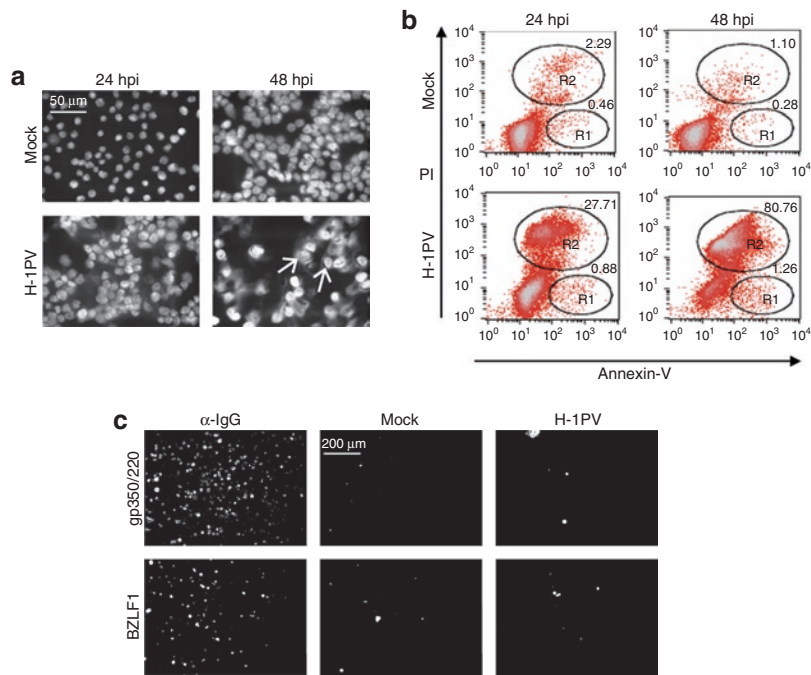


**Figure 4** Analysis of cytopathic changes and EBV reactivation in H-1PV-infected Namalwa cells. **(a,b)** H-1PV-induced cytopathic effects. Namalwa cells were stained with **(a)** Hoechst 33342 or **(b)** with propidium iodide (PI)/Annexin-V at 24 and 48 hours after infection (10 pfu/cell). **(a)** As described in the main text, most cells underwent necrosis, however, a few displayed apoptotic signs (arrows). **(b)** PI/Annexin-V staining was used to distinguish necrotic (R2) from apoptotic (R1) cell populations. **(c)** EBV reactivation. Akata cells were either H-1PV-infected (10 pfu/cell) or left untreated (Mock). At 48-hours postinfection (hpi), cells were harvested and immunostained against EBV BZLF1 or gp350/220 proteins. Akata cells treated with  $\alpha$ -IgG were used as a positive control.

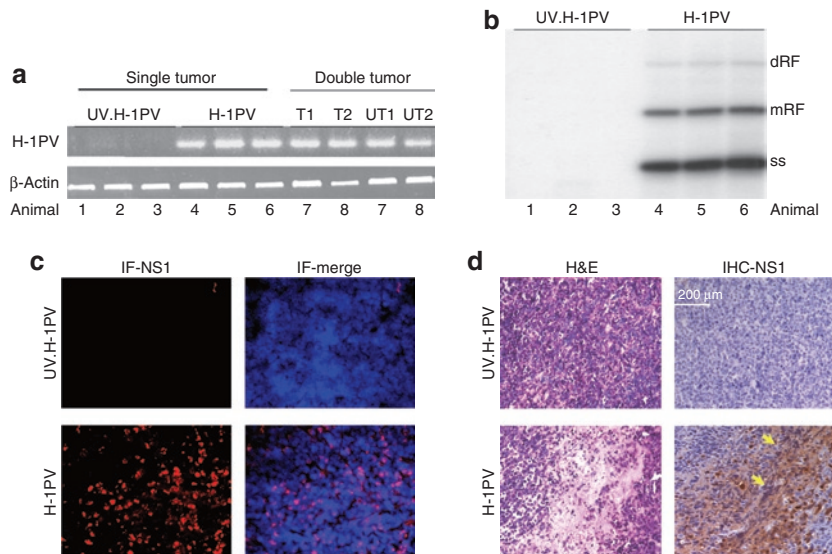


**Figure 5** H-1PV gene expression, DNA replication, and histopathological effects in Namalwa tumors. At day 7 after virus treatment, residual tumors were collected from SCID mice that harbored a single tumor injected with ultraviolet (UV)-inactivated H-1PV ( $n = 3$ ), a single tumor injected with infectious H-1PV ( $n = 3$ ), or two tumors of which one was inoculated with infectious H-1PV ( $n = 2$ ). **(a)** Total RNA was extracted and viral transcription was measured by semiquantitative RT-PCR with specific primers generating a 415-bp cDNA band.  $\beta$ -Actin expression served as matching control. T1,T2, treated tumor; UT1,UT2, untreated tumor. **(b)** Total DNA was isolated and subjected to Southern blot analysis using an H-1PV-specific probe detecting viral replicative forms. dRF, dimeric replicative form; mRF, monomeric replicative form; ss, single-stranded DNA. **(c)** Frozen tumor sections were labeled with fluorescent NS1-specific antibody (IF-NS1). **(d)** Paraffin-embedded tumor sections were subjected to hematoxylin–eosin staining (H&E) or processed for immunohistochemical detection of NS1 (IHC-NS1, arrows).

parvovirus treatment (**Figure 6a**), remaining disease-free for as long as 70 days after tumor initiation (**Figure 6b**).

These results encouraged us to evaluate H-1PV therapeutic potential under conditions mimicking late stages of lymphoma

development, a clinically relevant scenario (**Figure 6c,d**). Based on our data showing that H-1PV efficiently replicates in the Namalwa system, we treated mice with advanced disease with a tenfold lower dose of virus on day 28 post-tumor initiation. Tumor growth went

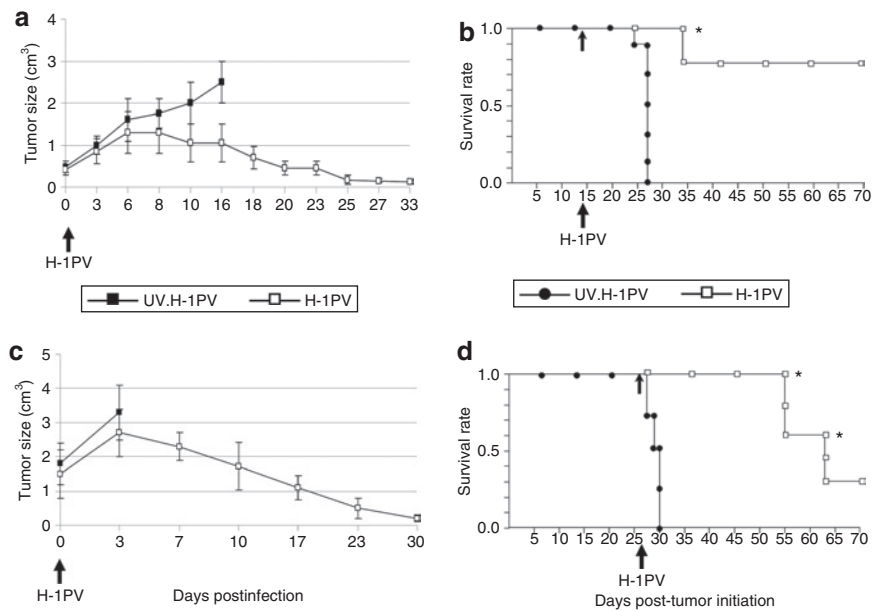


**Figure 6** H-1PV-induced suppression of lymphoma development in SCID mice. SCID mice carrying Namalwa cell implants were intratumorally injected with ultraviolet (UV)-inactivated (filled symbols) or infectious (open symbols) H-1PV at **(a,b)** day 14 or **(c,d)** 28 after implantation, when the size of tumors was  $0.5\text{ cm}^3$  or  $>1\text{ cm}^3$ , respectively. For each group ( $n = 10$ ), **(a,c)** the three-dimensional size of tumors was followed for 30 days post-treatment, and **(b,d)** the animals' survival was plotted as a Kaplan–Meier curve. The times of virus inoculation and of animal killing are indicated by arrows and asterisks, respectively.

on progressing in UV-inactivated H-1PV-treated control animals, which succumbed to the disease within the first 3 days following virus inoculation. In contrast, tumors in the infectious H-1PV-treated group started rapidly regressing 3–7 days postinfection (**Figure 6c**). Animals bearing macroscopically visible necrotic fields at the location of the original tumor (40%) were euthanized. Some (30%) of the surviving mice were killed for analytical purposes, confirming the absence of residual tumors. The remaining animals (30%) were disease-free and survived for a significantly prolonged ( $P < 0.01$ ) period of 70 days after tumor initiation (**Figure 6d**).

## DISCUSSION

NHLs are the fifth most common cancer in the United States and have one of the fastest growing incidence rates.<sup>20</sup> The development of a humanized monoclonal antibody against the pan-B cell marker CD20, rituximab, has recently raised hopes of improving the treatment outcome in NHL patients. However, limitations on rituximab application include selection of CD20-negative cell variants and induction of a profound B cell depletion for 6–8 months.<sup>21</sup> Despite the introduction of the previously described approaches and some other novel curative approaches, chemotherapy remains the main treatment modality for both NHLs and HL. Alternative, less toxic therapeutic strategies are therefore still needed for the efficient control of these lymphoid malignancies.

A novel, promising approach to cancer therapy consists in the application of oncolytic viruses able to induce selective destruction of tumor cells in direct and/or indirect ways. Among a number of viruses presently tested for their oncosuppressive capacity, rodent PVs have been reported to possess remarkable oncolytic properties.<sup>5,17</sup> Human cancer cell cultures derived from various carcinomas and melanomas have proved

to be targets for parvovirus replication and cytopathic effects.<sup>22</sup> It has recently been shown that the closely related rodent PVs H-1PV and minute virus of mice efficiently kill human glioblastoma cells both *in vitro* and *in vivo*.<sup>13,23</sup> Previous work by Faisst *et al.* has indicated that some BL-derived cell lines are permissive for H-1PV infection *in vitro*,<sup>18,19</sup> raising the possibility of this parvovirus being used in the fight against lymphoid tumors. This prompted us to extend the latter work by testing (i) the susceptibility of a wider panel of lymphoma cell lines to H-1PV infection, (ii) the specificity of parvoviral attack for malignant versus normal proliferating lymphocytes, and (iii) the capacity of H-1PV for activating distinct cell-death processes and killing rituximab-resistant lymphoma cells.

All lymphoma cell lines tested were sensitive to H-1PV infection. BL cells could be distinguished by their especially high responsiveness (with 80–100% of the culture being killed at 72 hours after inoculation of  $10\text{ pfu/cell}$ ), pointing to at least some NHLs as potential targets for parvovirus-based therapy. In keeping with this prospect, H-1PV was little toxic for stimulated normal B lymphocytes, whether bulk peripheral blood B cells or  $\text{CD19}^+/\text{CD27}^+$  (memory) B cells. H-1PV was equally efficient in killing both CD20-positive (rituximab-sensitive) and CD20-negative (rituximab-resistant, *e.g.*, Namalwa<sup>24</sup>) BL cell lines, and no change in the expression level of this marker could be detected after H-1PV infection (**Supplementary Figure S2**). These data raise hopes of H-1PV being of therapeutic value in lymphoma cases, which do not respond to rituximab treatment. Furthermore, BL cells sustained a productive H-1PV infection, thereby meeting the dependence of efficient virotherapy on successive rounds of infection through virus multiplication and spreading. In addition, H-1PV was also produced by some HL cell lines and might thus

be of value as an adjuvant to boost anti-HL immune responses. It is noteworthy that the HL-derived L540 cells were efficiently killed by H-1PV, although not being able to release virus progeny. Thus, sustaining a productive infection and cell killing could be dissociated; the latter being assigned to oncotoxic NS1 protein accumulation in infected cells.

Variations in the sensitivities of distinct lymphoid cell lines to H-1PV could not be traced back to the presence of EBV, as the BL-Elijah subclone that had lost the EBV genome kept its high sensitivity to parvovirus-induced death. Moreover, the RAMOS cell line derived from an EBV-negative lymphoma was efficiently killed by H-1PV and was among the strongest parvovirus producers. Therefore, sensitization to H-1PV does not require continuing expression of EBV proteins, arguing for the applicability of the parvovirus to the treatment of EBV-negative BLs. It has been shown that wild-type p53 expression compromises H-1PV-induced killing of hepatoma and leukemia-derived cell lines.<sup>12,25</sup> Interestingly, most of the BL-derived cell lines carry p53 mutations, in contrast to LCLs and HL cells.<sup>26,27</sup> This leads us to speculate that p53 mutations might contribute to sensitize BL cells to H-1PV-induced oncolysis. In addition, modulation of *c-myc* expression due to a *t*(8, 14) translocation, which is a hallmark of BL cells but is absent in HL-derived lines and LCLs, might impact on the outcome of parvovirus infection<sup>10</sup> and aggravate H-1PV cytopathic effects on the former cells.

The precise mechanism underlying parvovirus cytotoxicity is not yet fully understood. Depending on the tumor model considered, cell cycle arrest<sup>28</sup> and death through apoptosis,<sup>10</sup> necrosis,<sup>11</sup> or an autophagy-like process<sup>13</sup> have been observed. The mode of H-1PV-induced killing of lymphoma-derived cells was first characterized in this study. Parvovirus-infected Namalwa cell cultures were found to die predominantly through necrosis. This was apparent from nuclear swelling and spillover of nuclear DNA into the cytosol, and was confirmed by propidium iodide/Annexin-V staining. In agreement with these *in vitro* data, the tumors from H-1PV-treated animals showed extensive necrosis accompanied by NS1 protein expression.

An important issue was whether EBV-positive BL-cell death induced by the parvovirus might result from a break in EBV latency. This possibility needs to be considered as *in vitro* infection of EBV-positive cell lines (e.g., Akata) with human herpes virus 6 was reported to result in EBV reactivation.<sup>29</sup> A relationship between human cytomegalovirus infection and EBV reactivation has also been found.<sup>30</sup> This was, however, unlikely in our model system (Namalwa) as these cells carry two integrated copies of the virus<sup>31</sup> and may not be able to support EBV lytic replication. We still confirmed the absence of EBV reactivation in H-1PV-infected Namalwa and also Akata cells by monitoring the expression of EBV proteins that are characteristic of either early (BZLF1) or late (gp350/220) lytic cycle events. These assays failed to provide any evidence for EBV lytic replication after H-1PV infection of either cell line.

The Namalwa cell line was chosen for the establishment of an animal lymphoma model, based on the fact that these cells (i) were highly sensitive to H-1PV-induced oncolysis, (ii) efficiently produced infectious virus progeny, and (iii) have been reported to resist rituximab treatment,<sup>24</sup> thereby calling for alternative therapies. Tumors were initiated through subcutaneous Namalwa cell

engraftment in SCID mice, resulting in the rapid development of large tumors as previously reported for this model.<sup>32</sup> Lymphoma-bearing animals were subjected to a single intratumoral injection of infectious (treated group) or UV-inactivated (control group) H-1PV at an early (14 days) or late (28 days) time-point after tumor initiation. A striking tumor regression was observed in both early and late treatment protocols. Because SCID mice lack mature T and B lymphocytes, the direct oncolytic activity of H-1PV is likely to be mostly responsible for this effect. This was strongly supported by the histochemical analysis of virus-treated tumors showing the presence of large necrotic areas that stained positively for the viral cytotoxic NS1 protein. Besides H-1PV expression and replication within the neoplastic tissue, virus spreading to a distant tumor was detected. These features are consistent with the occurrence of a productive infection *in vivo*, as it was observed *in vitro*, thereby fulfilling the requirements for an efficient oncolytic effect. Indeed, H-1PV was successful in eradicating small (0.5 cm<sup>3</sup>) and large (>1 cm<sup>3</sup>) tumors. Even mice treated at an advanced stage of the disease showed striking survival prolongation. In contrast to the early treatment, the regression of advanced tumors upon therapy was characterized by necrotic involution, on account of which some animals were killed before completion of the experiment. The remainder survived until the end of the experiment (day 70 after tumor initiation).

Oncolytic viruses represent promising novel tools for the treatment of human tumors. Conditionally replicating adeno<sup>33</sup> and herpes simplex viruses,<sup>34</sup> reoviruses,<sup>35</sup> and live attenuated measles viruses<sup>36</sup> were reported to have significant potential as curative agents against B-lymphoblastic leukemia and lymphoma in preclinical settings. However, each oncolytic agent has its own virtues and limitations based on cellular receptor dependence, need for repeated virus inoculations, and size of the target tumor. Oncolytic PVs are advantageous in this regard as they recognize ubiquitous cellular receptors.<sup>5,17</sup> Furthermore, in this study a single parvovirus dose was sufficient to cause full regression of large tumors in the Namalwa xenograft model. Altogether, these data indicate that H-1PV deserves to be included in the arsenal of oncolytic viruses under consideration for lymphoma therapy.

## MATERIALS AND METHODS

**Cells.** Namalwa, Raji, and Elijah are human EBV-positive neoplastic BL-derived cell lines.<sup>37–39</sup> The EBV-negative subclone of Elijah cells was a kind gift from A.B. Rickinson (University of Birmingham, UK). RAMOS and RAMOS-EHRB are human Caucasian BL-derived cell lines, which are EBV-negative and EBV-positive, respectively.<sup>40</sup> RAMOS-AW is an EBV-positive cell line obtained by *in vitro* infection of RAMOS cells with EBV.<sup>40</sup> Akata cells, from a human Caucasian BL, are known to produce infectious EBV upon crosslinking surface IgG molecules with  $\alpha$ -IgG antibodies.<sup>41</sup> The JM and 2089 LCLs were established by *in vitro* infection of human donor peripheral blood B cells with EBV. Naive N17(8), Memory M9(8), Naive N3(20), and Memory M1(20) LCLs were established by *in vitro* EBV infection of purified naive and memory B cells isolated from the peripheral blood of two healthy donors (numbered 8 and 20, respectively). The EBV-negative HL-derived cell lines L540 (ref. 42) KM-H2 (ref. 43) and HDLM2 (ref. 44) were kindly provided by S. Joos (DKFZ, Heidelberg, Germany). All cell lines were maintained in Roswell Park Memorial Institute 1640 medium (Sigma, Hamburg, Germany) supplemented with 10% fetal calf serum, penicillin (100 U/ml), and streptomycin (100  $\mu$ g/ml). The established simian virus 40-transformed human newborn kidney cell line, NBK,



was grown in Eagle's minimum essential medium (Sigma) supplemented with 5% fetal calf serum. All cells were maintained at 37°C in a humidified 5% CO<sub>2</sub> incubator.

Peripheral blood mononuclear cells were isolated from the heparinized peripheral blood of healthy donors by differential centrifugation over Histopaque (Sigma). B lymphocytes were further negatively isolated by depletion of T cells, monocytes/macrophages, and NK cells (DynaB cell negative Isolation Kit; DynalBiotech, Hamburg, Germany), according to the manufacturer's instructions. The purity of the isolated population was assessed by fluorescence-activated cell sorting analysis and was confirmed to be over 80%. Lipopolysaccharide (Sigma) was applied at a final concentration 5 µg/ml.

**Flow cytometric analysis.** Flow cytometry was performed to detect changes in the proportion of memory B cells following H-1PV infection. Peripheral blood mononuclear cells were isolated and either H-1PV-infected (10 pfu/cell) or mock treated. At 48 hpi, cells were stained with anti-CD19-FITC, anti-CD27-PE (Becton Dickinson, Heidelberg, Germany), and anti-CD20-APC (Immunotools, Friesoythe, Germany). Triple-color analysis of B cell surface molecule expression was performed using a FACSCalibur (Becton Dickinson). The subpopulation of memory B lymphocytes (CD19<sup>+</sup>/CD27<sup>+</sup>) was determined relative to the whole CD20<sup>+</sup>/CD19<sup>+</sup> B-cell population.

**Virus production and titration.** Wild-type H-1PV was produced by infecting NBK cells, purified through iodixanol gradient centrifugation and dialyzed against Ringer solution. Virus stocks were titered using a standard plaque assay, and titers were expressed as pfu/ml. The recombinant virus expressing EGFP (chi-H-1PV/EGFP) was generated as previously described<sup>45</sup> and kindly provided by C. Dinsart (DKFZ). Inactivated virus used as control in animal studies was prepared by H-1PV exposure to UV light (185–254 nm for 6 hours) resulting in loss of infectivity, as confirmed by infecting NBK cells with serial dilutions of the irradiated virus.

For the titration of H-1PV infectious progeny released from the lymphoma cell lines, a modified replication assay was used, as previously described.<sup>19</sup> Briefly, cultures were infected at 0.1 pfu/cell and harvested at 12 and 72 hpi. The samples were subjected to three freeze-thaw cycles, and serial dilutions were used to infect NBK monolayers. At 48 hpi, infected NBK cells were transferred onto nitrocellulose filters (Whatman; Schleicher & Schuell, Dassel, Germany). After DNA denaturation and neutralization, filters were hybridized with a <sup>32</sup>P-labeled H-1PV DNA-specific probe. The centers of viral replication were counted, and virus titer was expressed as center-forming units/ml.

**Cytotoxicity assays.** The cells were seeded in 96-well culture plates (Nunclon, Nunc, Germany) at 2 × 10<sup>4</sup> cells/well, incubated for 6 hours and inoculated with H-1PV at various multiplicities of infection. At 24, 48, and 72 hpi, the fraction of viable versus dead cells was determined using the Trypan blue dye (Fluka Chemie, Deisenhofen, Germany) exclusion test. Data were presented as percentage of dead cells relative to the mock-treated control. For assessment of the survival of H-1PV-infected normal peripheral blood B cells, the CellTiter96 Aqueous One Solution Cell Proliferation (methyl tetrazolium salt) Assay (Promega, Mannheim, Germany) was additionally used, according to the manufacturer's instructions.

**Immunostaining.** For the detection of EBV replicative cycle activation, 1.5 × 10<sup>6</sup> Akata or Namalwa cells were seeded in 10-cm dishes (Nunclon) and either H-1PV-infected (10 pfu/cell) or mock treated. In order to induce lytic EBV replication, 4 × 10<sup>6</sup> Akata cells (positive control) were treated with α-IgG antibody (Cappel Laboratories, Malvern, PA), as previously described.<sup>41</sup> At 48 hpi, cells were harvested, washed, and resuspended in 50-µl phosphate-buffered saline (PBS). The cell suspension was spread onto a slide and fixed for 20 minutes at room temperature with either acetone (for staining against EBV gp350/220) or 4% paraformaldehyde followed by a 2-minute permeabilization with 0.1% Triton X-100

(for staining against EBV BZLF1). Slides were stained for 30 minutes at 37°C in the dark with the following primary antibodies: mouse monoclonal anti-BZLF1 antibody (sc-53904; Santa Cruz Biotechnology, Santa Cruz, CA), 1:500 in 10% heat-inactivated goat serum in PBS (PBS-Hings), or mouse monoclonal anti-gp350/220 antibody (HB168, ATCC), 1:250 in PBS-Hings. The secondary antibody was cyanine 3-coupled goat anti-mouse IgG (Dianova, Hamburg, Germany).

For the detection of H-1PV NS1 protein in tumors, frozen tissue samples from control and treated animals were cut into 15-µm sections and placed on poly-L-lysine-coated microscope slides (Roth, Karlsruhe, Germany). After Triton X-100 permeabilization for 20 minutes, slides were incubated with 5% PBS-Hings for 1 hour at room temperature to block nonspecific binding. Mouse monoclonal NS1-specific antibody 3D9, a kind gift from N. Salomé (DKFZ), was added (1:50 in PBS) for 18 hours at 4°C. After a washing step, slides were further incubated with the secondary antibody, cyanine 3-conjugated goat antimouse IgG (Jackson ImmunoResearch, West Grove, PA), 1:500 in PBS, for 3 hours at room temperature. Slides were embedded with 4',6-diamidino-2-phenylindole-containing mounting medium (VECTASHIELD; Vector Laboratories, Burlingame, CA). Immunofluorescence was measured using a Leica DMRBE fluorescent microscope (Leica, Bensheim, Germany) and the analySIS software (Olympus, Germany).

**Immunohistochemistry.** Paraffin wax-embedded tumor sections were dewaxed with xylene and rehydrated through graded alcohol solutions. Endogenous peroxidase activity was quenched with 0.3% hydrogen peroxide in methanol. To block the nonspecific binding, slides were treated with nonimmune normal rabbit serum (Dako, Zurich, Switzerland) for 1 hour. After overnight incubation (4°C) with the NS1-specific 3D9 antibody (1:50), slides were washed and treated with rabbit antimouse horseradish peroxidase-labeled secondary antibody (1/200; Sigma), developed using the Dako Envision + System (Dako) and counterstained with Mayer's hematoxylin.

**H-1PV expression and DNA replication in vivo.** For the detection of virus transcription, total RNA was extracted from residual tumors of H-1PV-treated mice using TRIzol Reagent (Invitrogen, Karlsruhe, Germany), according to the manufacturer's instructions. RNA was reverse-transcribed into cDNA and quantified by reverse transcription-PCR, as previously described.<sup>46</sup> Virus transcripts were detected as 512- and 415-bp PCR fragments, depending on the excision of the small intron. The following primer pair was used: 5'-TCAATGCGCTCACCATCTCTG-3' (forward) and 5'-TCGTAGGCTTCGTCGTGTCT-3' (reverse). Human β-actin primers have been previously described.<sup>46</sup>

H-1PV replicative forms were detected by Southern blotting. Briefly, DNA was extracted from treated animals' residual tumor samples using the modified Hirt's method,<sup>47</sup> fractionated through 0.8% agarose gel electrophoresis, blotted onto a Hybond N nitrocellulose membrane (Amersham, Freiburg, Germany) and hybridized to a <sup>32</sup>P-labeled H-1PV DNA-specific probe.

**Animal studies.** Four to six-week-old female SCID mice (C.B-17/IcrHanHsd-scid) were purchased from Harlan (Gannat, France) and housed in a pathogen-free biocontainment facility. All manipulations were performed in accordance with the recommendations of the National Ethics Committee. For the generation of tumors, 5 × 10<sup>6</sup> Namalwa cells in 100-µl PBS were injected subcutaneously into the hind flank. After palpable tumors have appeared, mice received a single intratumoral injection of infectious H-1PV (treated group) or were equivalently inoculated with UV-inactivated virus (control group). The three-dimensional tumor size was measured at regular intervals using a caliper. Mice were killed if any complications due to excess tumor burden or development of macroscopically visible necrotic areas after H-1PV treatment were observed, as well as for analytical purposes. Survival curves were plotted according to the Kaplan-Meier method.

**Statistical methods.** *In vitro* cytotoxicity data represent mean values with standard deviations from three independent experiments. For the *in vivo* mortality data assessment, experimental groups were compared according to the logarithm-rank test, using the GraphPad InStat 2.05 software for Macintosh (San Diego, CA).

## SUPPLEMENTARY MATERIAL

**Figure S1.** EGFP expression after chi-H-1PV/EGFP infection of transformed versus normal B lymphocytes.

**Figure S2.** CD20 expression in BL cells.

## ACKNOWLEDGMENTS

We express our gratitude to Barbara Leuchs (DKFZ, Heidelberg, Germany) for providing purified wild-type H-1PV. We thank Alexia Herrmann, Melanie Krämmer (DKFZ, Heidelberg, Germany), and Brunhilde Bentzinger (University of Heidelberg, Heidelberg, Germany) for their excellent technical assistance. We are grateful to Irene Joab and the French network "Herpesviruses and Cancer," as well as to Martina Seiffert (DKFZ, Heidelberg, Germany) for helpful discussions. A.L.A. was supported by a guest researcher fellowship from the DKFZ on leave from the Stephan Angeloff Institute of Microbiology, Sofia, Bulgaria. The authors have no conflicts of interest and have nothing to disclose.

## REFERENCES

- Rickinson, AB and Kieff, E (1996). Epstein-Barr virus. In: Fields, BN, Knipe, DM and Howley, PM (eds). *Fields Virology*, 3rd edn., Lippincott-Raven: Philadelphia, PA. pp. 2397–2446.
- Delecluse, HJ, Feederle, R, O'Sullivan, B and Taniere, P (2007). Epstein-Barr virus-associated tumours: an update for the attention of the working pathologist. *J Clin Pathol* **60**: 1358–1364.
- Abali, H, Urün, Y, Oksüzoglu, B, Budakoglu, B, Yildirim, N, Güler, T *et al.* (2008). Comparison of ICE (ifosfamide-carboplatin-etoposide) versus DHAP (cytosine arabinoside-cisplatin-dexamethasone) as salvage chemotherapy in patients with relapsed or refractory lymphoma. *Cancer Invest* **26**: 401–406.
- Milpied, N, Vasseur, B, Parquet, N, Garnier, JL, Antoine, C, Quartier, P *et al.* (2000). Humanized anti-CD20 monoclonal antibody (Rituximab) in post transplant B-lymphoproliferative disorder: a retrospective analysis on 32 patients. *Ann Oncol* **11** (Suppl. 1): 113–116.
- Geletneky, K, Herrero Y Calle, M, Rommelaere, J and Schlehofer, JR (2005). Oncolytic potential of rodent parvoviruses for cancer therapy in humans: a brief review. *J Vet Med B Infect Dis Vet Public Health* **52**: 327–330.
- Bashir, T, Horlein, R, Rommelaere, J and Willwand, K (2000). Cyclin A activates the DNA polymerase delta-dependent elongation machinery *in vitro*: A parvovirus DNA replication model. *Proc Natl Acad Sci USA* **97**: 5522–5527.
- Perros, M, Deleu, L, Vanacker, JM, Kherrouche, Z, Spruyt, N, Faist, S *et al.* (1995). Upstream CREs participate in the basal activity of minute virus of mice promoter P4 and in its stimulation in ras-transformed cells. *J Virol* **69**: 5506–5515.
- Mousset, S, Ouadrhiri, Y, Caillet-Fauquet, P and Rommelaere, J (1994). The cytotoxicity of the autonomous parvovirus minute virus of mice nonstructural proteins in FR3T3 rat cells depends on oncogene expression. *J Virol* **68**: 6446–6453.
- Caillet-Fauquet, P, Perros, M, Brandenburger, A, Spegelaere, P and Rommelaere, J (1990). Programmed killing of human cells by means of an inducible clone of parvoviral genes encoding non-structural proteins. *EMBO J* **9**: 2989–2995.
- Rayet, B, Lopez-Guerrero, JA, Rommelaere, J and Dinsart, C (1998). Induction of programmed cell death by parvovirus H-1 in U937 cells: connection with the tumor necrosis factor alpha signalling pathway. *J Virol* **72**: 8893–8903.
- Ran, Z, Rayet, B, Rommelaere, J and Faist, S (1999). Parvovirus H-1-induced cell death: influence of intracellular NAD consumption on the regulation of necrosis and apoptosis. *Virus Res* **65**: 161–174.
- Moehler, M, Blechacz, B, Weiskopf, N, Zeidler, M, Stremmel, W, Rommelaere, J *et al.* (2001). Effective infection, apoptotic cell killing and gene transfer of human hepatoma cells but not primary hepatocytes by parvovirus H1 and derived vectors. *Cancer Gene Ther* **8**: 158–167.
- Di Piazza, M, Mader, C, Geletneky, K, Herrero Y Calle, M, Weber, E, Schlehofer, J *et al.* (2007). Cytosolic activation of cathepsins mediates parvovirus H-1-induced killing of cisplatin and TRAIL-resistant glioma cells. *J Virol* **81**: 4186–4198.
- Faist, S, Guittard, D, Benner, A, Cesbron, JY, Schlehofer, JR, Rommelaere, J *et al.* (1998). Dose-dependent regression of HeLa cell-derived tumours in SCID mice after parvovirus H-1 infection. *Int J Cancer* **75**: 584–589.
- Dupressoir, T, Vanacker, JM, Cornelis, JJ, Duponchel, N and Rommelaere, J (1989). Inhibition by parvovirus H-1 of the formation of tumors in nude mice and colonies *in vitro* by transformed human mammary epithelial cells. *Cancer Res* **49**: 3203–3208.
- Angelova, AL, Arahamian, M, Grekova, SP, Hajri, A, Leuchs, B, Giese, NA *et al.* (2009). Improvement of gemcitabine-based therapy of pancreatic carcinoma by means of oncolytic parvovirus H-1PV. *Clin Cancer Res* **15**: 511–519.
- Rommelaere, J and Cornelis, JJ (1991). Antineoplastic activity of parvoviruses. *J Virol Methods* **33**: 233–251.
- Faist, S, Schlehofer, JR and zur Hausen, H (1989). Transformation of human cells by oncogenic viruses supports permissiveness for parvovirus H-1 propagation. *J Virol* **63**: 2152–2158.
- Faist, S, Bartnitzke, S, Schlehofer, JR and zur Hausen, H (1990). Persistence of parvovirus H-1 DNA in human B- and T-lymphoma cells. *Virus Res* **16**: 211–223.
- O'Leary, M, Sheaffer, J, Keller, F, Shu, X-O, and Cheson, B (2006). Lymphoma and reticuloendothelial neoplasms. In: Bleyer, A, O'Leary, M, Barr, R, Ries, LAG (eds). *Cancer Epidemiology in Older Adolescents and Young Adults 15 to 29 Years of Age. Including SEER Incidence and Survival: 1972–2000* [National Institutes of Health Publication No. 06-5767]. National Cancer Institute: Bethesda, MD.
- Heslop, HE (2005). Biology and treatment of Epstein-Barr virus-associated non-Hodgkin lymphomas. *Hematology Am Soc Hematol Educ Program*: 260–266.
- Wetzel, K, Struyf, S, Van Damme, J, Kayser, T, Vecchi, A, Sozzani, S *et al.* (2007). MCP-3 (CCL7) delivered by parvovirus MVMP reduces tumorigenicity of mouse melanoma cells through activation of T lymphocytes and NK cells. *Int J Cancer* **120**: 1364–1371.
- Wollmann, G, Tattersall, P and van den Pol, AN (2005). Targeting human glioblastoma cells: comparison of nine viruses with oncolytic potential. *J Virol* **79**: 6005–6022.
- Ghetie, MA, Bright, H and Vitetta, ES (2001). Homodimers but not monomers of Rituxan (chimeric anti-CD20) induce apoptosis in human B-lymphoma cells and synergize with a chemotherapeutic agent and an immunotoxin. *Blood* **97**: 1392–1398.
- Telerman, A, Tuynder, M, Dupressoir, T, Robaye, B, Sigaux, F, Shaullian, E *et al.* (1993). A model for tumor suppression using H-1 parvovirus. *Proc Natl Acad Sci USA* **90**: 8702–8706.
- Farrell, PJ, Allan, GJ, Shanahan, F, Voudsen, KH and Crook, T (1991). p53 is frequently mutated in Burkitt's lymphoma cell lines. *EMBO J* **10**: 2879–2887.
- Ichikawa, A, Kinoshita, T, Watanabe, T, Kato, H, Nagai, H, Tsushita, K *et al.* (1997). Mutations of the p53 gene as a prognostic factor in aggressive B-cell lymphoma. *N Engl J Med* **337**: 529–534.
- Op De Beeck, A, Anouja, F, Mousset, S, Rommelaere, J and Caillet-Fauquet, P (1995). The non-structural proteins of the autonomous parvovirus minute virus of mice interfere with the cell cycle, inducing accumulation in G2. *Cell Growth Differ* **6**: 781–787.
- Flamand, L, Stefanescu, I, Ablashi, DV and Menezes, J (1993). Activation of the Epstein-Barr virus replicative cycle by human herpesvirus 6. *J Virol* **67**: 6768–6777.
- Arceas, R and Widen, RH (2002). Epstein-Barr virus reactivation after superinfection of the BJAB-B1 and P3HR-1 cell lines with cytomegalovirus. *BMC Microbiol* **2**: 20.
- Henderson, A, Ripley, S, Heller, M and Kieff, E (1983). Chromosome site for Epstein-Barr virus DNA in a Burkitt tumor cell line and in lymphocytes growth-transformed *in vitro*. *Proc Natl Acad Sci USA* **80**: 1987–1991.
- Hudson, WA, Li, Q, Le, C and Kersey, JH (1998). Xenotransplantation of human lymphoid malignancies is optimized in mice with multiple immunologic defects. *Leukemia* **12**: 2029–2033.
- Qian, W, Liu, J, Tong, Y, Yan, S, Yang, C, Yang, M *et al.* (2008). Enhanced antitumor activity by a selective conditionally replicating adenovirus combining with MDA-7/interleukin-24 for B-lymphoblastic leukemia via induction of apoptosis. *Leukemia* **22**: 361–369.
- Farassati, F, Atanaskova, N, Raffel, C, Johnston, P and Lee, P (2004). Ras signalling as a marker for application of oncolytic herpes mutant against lymphoma. *Mol Ther* **9** (Suppl. 1): S26.
- Alain, T, Hirasawa, K, Pon, KJ, Nishikawa, SG, Urbanski, SJ, Auer, Y *et al.* (2002). Reovirus therapy of lymphoid malignancies. *Blood* **100**: 4146–4153.
- Grote, D, Russell, SJ, Cornu, TI, Cattaneo, R, Vile, R, Poland, GA *et al.* (2001). Live attenuated measles virus induces regression of human lymphoma xenografts in immunodeficient mice. *Blood* **97**: 3746–3754.
- Klein, F, Ricketts, RT, Jones, WI, DeArmon, IA, Temple, MJ, Zoon, KC *et al.* (1979). Large-scale production and concentration of human lymphoid interferon. *Antimicrob Agents Chemother* **15**: 420–427.
- Pulvertaft, JV (1964). Cytology of Burkitt's tumour (African lymphoma). *Lancet* **1**: 238–240.
- Rowe, M, Rooney, CM, Rickinson, AB, Lenoir, GM, Rupani, H, Moss, DJ *et al.* (1985). Distinctions between endemic and sporadic forms of Epstein-Barr virus-positive Burkitt's lymphoma. *Int J Cancer* **35**: 435–441.
- Klein, G, Giovanella, B, Westman, A, Stehlin, JS and Mumford, D (1975). An EBV-genome-negative cell line established from an American Burkitt lymphoma; receptor characteristics. EBV infectibility and permanent conversion into EBV-positive sublines by *in vitro* infection. *Intervirology* **5**: 319–334.
- Takada, K, Horinouchi, K, Ono, Y, Aya, T, Osato, T, Takahashi, M *et al.* (1991). An Epstein-Barr virus-producer line Akata: establishment of the cell line and analysis of viral DNA. *Virus Genes* **5**: 147–156.
- Fonatsch, C, Diehl, V, Schaadt, M, Burrichter, H and Kirchner, HH (1986). Cytogenetic investigations in Hodgkin's disease: I. Involvement of specific chromosomes in marker formation. *Cancer Genet Cytogenet* **20**: 39–52.
- Uehira, K, Amakawa, R, Ito, T, Uehira, T, Ozaki, Y, Shimizu, T *et al.* (2001). A Hodgkin's disease cell line, KM-H2, shows biphenotypic features of dendritic cells and B cells. *Int J Hematol* **73**: 236–244.
- Drexler, HG, Gaedicke, G, Lok, MS, Diehl, V and Minowada, J (1986). Hodgkin's disease derived cell lines HDLM-2 and L-428: comparison of morphology, immunological and isoenzyme profiles. *Leuk Res* **10**: 487–500.
- Wrzesinski, C, Tesfay, L, Salomé, N, Jauniaux, JC, Rommelaere, J, Cornelis, J *et al.* (2003). Chimeric and pseudotyped parvoviruses minimize the contamination of recombinant stocks with replication-competent viruses and identify a DNA sequence that restricts parvovirus H-1 in mouse cells. *J Virol* **77**: 3851–3858.
- Giese, NA, Raykov, Z, DeMartino, L, Vecchi, A, Sozzani, S, Dinsart, C *et al.* (2002). Suppression of metastatic hemangiosarcoma by a parvovirus MVMP vector transducing the IP-10 chemokine into immunocompetent mice. *Cancer Gene Ther* **9**: 432–442.
- Dupont, F, Tenenbaum, L, Guo, LP, Spegelaere, P, Zeicher, M and Rommelaere, J (1994). Use of an autonomous parvovirus vector for selective transfer of a foreign gene into transformed human cells of different tissue origins and its expression therein. *J Virol* **68**: 1397–1406.